

CO-OFDM DSP Channel Estimation

Pranav Ravikumar, Arunabha Bera, Vijay K. Mehra, and Anand Kumar

Abstract—This paper solves the Non Linear Schrodinger Equation using the Split Step Fourier method for modeling an optical fiber. The model generates a complex wave of optical pulses and using the results obtained two graphs namely Loss versus Wavelength and Dispersion versus Wavelength are generated. Taking Chromatic Dispersion and Polarization Mode Dispersion losses into account, the graphs generated are compared with the graphs formulated by JDS Uniphase Corporation which uses standard values of dispersion for optical fibers. The graphs generated when compared with the JDS Uniphase Corporation plots were found to be more or less similar thus verifying that the model proposed is right. MATLAB software was used for doing the modeling.

Keywords—Modulation, Non Linear Schrodinger Equation, Optical fiber, Split Step Fourier Method.

I. INTRODUCTION

ORTHOGONAL Frequency Division Multiplexing (OFDM) is a modulation scheme, which is the fundamental principle of many Wireless Communications. In recent years there is a growing interest to apply OFDM in Optical Communications to support very high-speed data transmission. The application of OFDM in optical communication is enabled because of rapid strides in semiconductor technology that allow high speed switching to perform DSP(Digital Signal Processing) calculations required for OFDM processing in silicon.

Coherent optical OFDM (CO-OFDM) is a modulation scheme widely studied for terabit rate optical networks. The high data rate involved increases the complexity of the CO-OFDM receiver design which is responsible to demodulate the received signal which suffer from degradations due to optical noise, PMD (polarization mode dispersion), chromatic dispersion (CD), PDL (polarization dependent loss) and fiber non-linearity's.

Channel estimation is one of the important components in a receive chain to compensate or neutralize the effects of degradation the signal suffers during transmission. OFDM schemes widely adopt pilot-based channel estimation techniques where the amplitude and phase of the received pilot signal is compared against its expected form to evaluate the

effects of the channel. Pilots for different carriers are extracted by performing DFT over the received OFDM signal.

II. OFDM IN OPTICAL COMMUNICATIONS

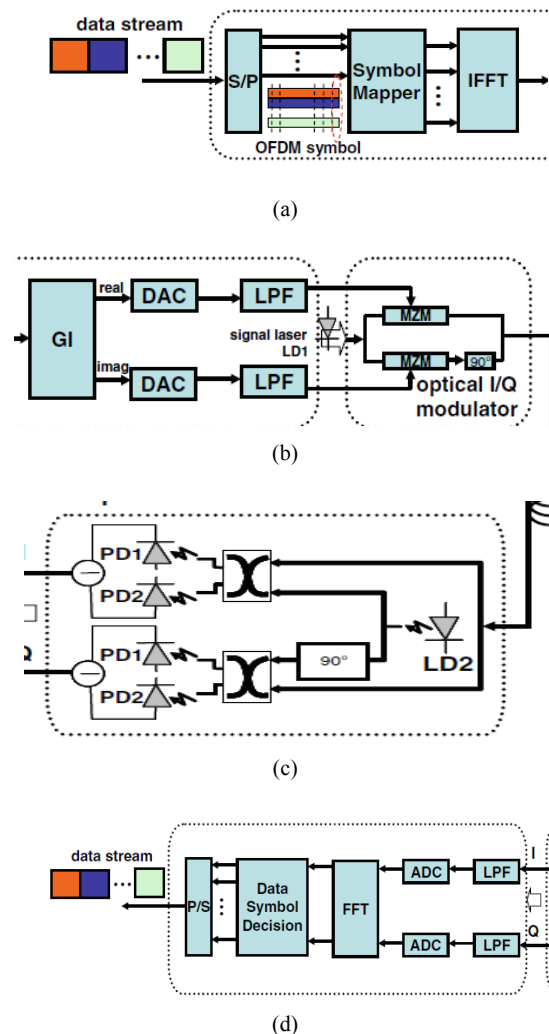


Fig. 1 (a) Diagram of a typical OFDM Transmitter (b) Diagram of an RF to Optical Up Converter (c) Diagram of an Optical to RF down Converter (d) Diagram of a typical OFDM Receiver [1]

The figures collectively show the conceptual diagram of a typical Coherent Optical OFDM System setup. It contains five basic functional blocks, RF OFDM signal transmitter, RF to Optical (RTO) Up-Converter, Fiber links, the Optical to RF (OTR) Down-Converter, and the RF OFDM receiver. This setup can also be used for a single-carrier scheme, in which

Pranav Ravikumar is a final year student pursuing his Electronics and Communication Engineering in BITS Pilani Dubai, Dubai 345055 UAE. (Phone: +971554962351; e-mail: f2009203@bits-dubai.ac.ae).

Vijay K. Mehra is the founder of the company iCoreTec and Arunabha Bera is the Principal Engineer in the same company located in Whitefield, Bangalore, Karnataka, 560037, India. They can be reached at vijay@icorettec.com and arunabha.bera@gmail.com respectively. This work is being done as part of research collaboration between iCoreTec and BITS Pilani, Dubai Campus.

Dr. Anand Kumar is with the department of Electrical and Electronics Engineering, BITS Pilani, Dubai Campus, Dubai International Academic City, Dubai, UAE. He can be reached at akumar@bits-dubai.ac.ae.

the DSP (Digital Signal Processing) part in the transmitter and receiver needs to be modified, while all the hardware setup remains the same.

In the RF OFDM transmitter, the input binary data is first split into multiple parallel branches. This procedure is referred to as “serial-to-parallel” conversion. The number of multiple branches equals the number of subcarriers. Then the converted signal is mapped onto various modulation formats, such as Phase-Shift Keying (PSK), Quadrature Amplitude Modulation (QAM), etc. The IDFT will convert the mapped signal from the frequency domain into the time domain. A two-dimensional complex signal is used to carry the information. Digital-to-Analogue Signal converters (DACs) are used to convert the time-domain digital signal to analogue signal.

At the RF to Optical Up-Converter, the baseband OFDM signal $S_B(t)$ is up shifted onto the optical domain using an optical I/Q modulator, which is comprised of two Mach-Zehnder modulators (MZMs) within a 90 degree optical phase shifter. The up converted OFDM signal in optical domain is given by

$$E(t) = \exp(j\omega_{LD1}t + \varphi_{LD1}) S_B(t) \quad (1)$$

When the optical signal is fed into the Optical to RF down converter, the optical signal $E'(t)$ is then mixed with a local laser at a frequency of ω_{LD2} and a phase of φ_{LD2} . Assuming the frequency and phase difference between the transmitter and receiver lasers to be

$$\Delta\omega = \omega_{LD1} - \omega_{LD2}, \Delta\varphi = \varphi_{LD1} - \varphi_{LD2} \quad (2)$$

Then the received RF OFDM signal can be expressed as

$$r(t) = \exp(j\Delta\omega t + \Delta\varphi) S_B(t) \otimes h(t) \quad (3)$$

In the RF OFDM receiver, the down-converted RF signal is first sampled by high speed analogue-to-digital converter (ADC). The typical OFDM signal processing comprises of five steps namely Window Synchronization, Frequency Synchronization, Discrete Fourier Transform, Channel Estimation and Phase Noise Estimation.

Window Synchronization aims to locate the beginning and end of an OFDM symbol correctly. A certain amount of frequency offset can be synchronized by a similar method, namely, the frequency offset can be estimated from the phase difference between two identical patterns with a known time offset. After Window Synchronization, the OFDM signal is partitioned into blocks each containing a complete OFDM symbol. DFT is used to convert each block of OFDM signal from time domain to frequency domain. Then the channel and phase noise estimations are performed in the frequency domain using training symbols and pilot subcarriers respectively.

OFDM is used extensively in broadband wired and wireless communication systems because it is an effective solution to

Inter Symbol Interference (ISI) caused by a dispersive channel. This becomes increasingly important as data rates increase to the point where, schemes like Quadrature amplitude modulation (QAM) or NRZ are used; their received signal at any time depends on multiple transmitted symbols. In contrast, the complexity of OFDM, and of systems using serial modulation and frequency domain equalization, scale well as data rates and dispersion increase[2]–[4]. While many details of OFDM systems are very complex, the basic concept of OFDM is quite simple [5]–[7]. Data is transmitted in parallel on a number of different frequencies, and as a result their symbol period is much longer than for a serial system with the same total data rate. Because the symbol period is longer, ISI affects at most one symbol, and equalization is simplified. In most OFDM implementations any residual ISI is removed by using a form of guard interval called a cyclic prefix.

In [8], Kahn and Barry explain why the many optical modes present at the receiver result in optical wireless systems being linear in intensity. Thus the modulating signal must be both real and positive, whereas baseband OFDM signals are generally complex and bipolar.

There are two forms of unipolar OFDM: DC-biased optical OFDM (DCO-OFDM) [9], [10] and asymmetrically clipped OFDM (ACO-OFDM) [11], [12]. In the former DC bias is added to the signal, however because of the large PAPR ratio of OFDM, even with a large bias some negative peaks of the signal will be clipped and the resulting distortion limits performance [12]. In ACO-OFDM the bipolar OFDM signal is clipped at the zero level: all negative going signals are removed [12] except for extremely large constellations ACO-OFDM requires a lower average optical power for a given Bit Error Rate and data rate than DCO-OFDM [13]. DCO-OFDM has been demonstrated experimentally for optical wireless [14], multimode fiber [15] and plastic optical fiber [16]. A number of simulation studies examine the performance of DCO-OFDM in more detail [17], and how adaptive modulation can be used to improve performance [18].

In single mode optical fiber systems the best way to achieve linearity between the transmitter IFFT input and the receiver FFT output is to map each discrete OFDM subcarrier frequency in the baseband electrical domain to a single discrete frequency in the optical domain. This is achieved by using linear field modulation, so that there is a linear relationship between the optical field of the transmitted signal and the OFDM baseband signal [19]. At the receiver the OFDM signal is mixed with a component at the optical carrier frequency and the signal detected from the carrier signal mixing products. The component at the optical carrier frequency can either be transmitted with the OFDM signal as in direct-detection optical OFDM (DD-OOFDM) [20] or coherent detection can be used where the received signal is mixed with a locally generated carrier signal as in coherent optical OFDM (CO-OFDM) [21]. Both techniques have advantages. DD-OOFDM has a simple receiver, but some optical frequencies must be unused if unwanted mixing products are not to cause interference. This is usually achieved by inserting a guard band between the optical carrier and the

OFDM subcarriers. A laser is required for the Coherent OFDM at the receiver to generate the carrier locally, and is more sensitive to phase noise. There is currently extensive research into the performance of both systems and on techniques to mitigate the disadvantages of each [22]. The modeling of the optical fiber connecting the RF to Optical up Converter and the Optical to RF down Converter is described in detail in this paper.

III. NON LINEAR SCHRODINGER EQUATION

In optics, the Non Linear Schrödinger equation occurs in the Manakov system, a model of wave propagation in fiber optics. Evolution of the slow varying complex envelope $A(z, t)$ of the optical pulses along a single mode optical fiber is governed by the well-known Non Linear Schrodinger Equation (NLSE) [23]:

$$\frac{\partial A(z,t)}{\partial z} + \frac{\alpha}{2} A(z,t) + \beta_1 \frac{\partial A(z,t)}{\partial t} + j\beta_2 \frac{\partial^2 A(z,t)}{\partial t^2} - \frac{1}{6} \beta_3 \frac{\partial^3 A(z,t)}{\partial t^3} = -j\gamma |A(z,t)|^2 A(z,t) \quad (4)$$

where z is the spatial longitudinal coordinate, α represents Fiber Attenuation, β_1 refers to Differential Group Delay (DGD), β_2 and β_3 are defined as 2nd and 3rd order factors of the Group Velocity Dispersion (GVD) and γ is the nonlinear coefficient.

IV. SPLIT STEP FOURIER METHOD

Solutions of the NLSE and hence the model of pulse propagation in a single mode optical fiber is numerically solved by using the popular approach of the Split Step Fourier method (SSFM) [5] in which the fiber length is divided into a large number of segments of small step size δz .

In practice, dispersion and nonlinearity are mutually interactive while the optical pulses propagate through the fiber. However, the SSFM assumes that over a small length δz , the effects of dispersion and the nonlinearity on the propagating optical field are independent. Thus, in SSFM, the linear operator representing the effects of fiber dispersion and attenuation and the nonlinearity operator taking into account fiber nonlinearities are defined separately as [23],

$$\hat{D} = -\frac{i\beta_2}{2} \frac{\partial^2}{\partial T^2} + \frac{\beta_3}{6} \frac{\partial^3}{\partial T^3} - \frac{\alpha}{2} \quad (5)$$

$$\hat{N} = i\gamma |A|^2 \quad (6)$$

where A replaces $A(z, t)$ for simpler notation and $T = (t-z)/v_g$ is the reference time frame moving at the group velocity. Thus the NLSE can be rewritten [23] as

$$\frac{\partial A}{\partial z} = (\hat{D} + \hat{N})A$$

and the complex amplitudes of optical pulses propagating from z to $z+\delta z$ is calculated using the approximation as given [23].

$$A(z + \delta z, T) \approx \exp(h\hat{D}) \exp(h\hat{N}) A(z, t)$$

The NLSE is accurate to the second order in the step size δz . The accuracy of SSFM can be improved by including the effect of the nonlinearity in middle of the segment rather than at the segment boundary. The equation can now be further modified [23] as

$$A(z + \delta z, T) \approx \exp\left(\frac{\delta z}{2} \hat{D}\right) \exp\left(\int_z^{z+\delta z} \hat{N}(z') dz'\right) \exp\left(\frac{\delta z}{2} \hat{D}\right) A(z, t)$$

This method is accurate to the third order in step size δz . The optical pulse is propagated down segment from segment in two stages at each step. The pulse passes through the first linear operator (step of $\delta z/2$) with dispersion effects taken into account only. The nonlinearity is calculated in the middle of the segment. It is noted that the nonlinearity effects is considered as over the whole segment. Then at $z + \delta z/2$, the pulse propagates through the remaining $\delta z/2$ distance of the linear operator. The process continues repetitively in executive segments δz until the end of the fiber. This method requires the careful selection of step sizes δz to reserve the required accuracy.

V. SIMULATION RESULTS

The first and foremost step is to model an optical fiber. This requires solving the Non Linear Schrodinger Equation numerically. The method used here to solve the NLSE is the Split Step Fourier Method. MATLAB was used in the simulations and the results are discussed here.

A. Generation of Input Optical Pulse

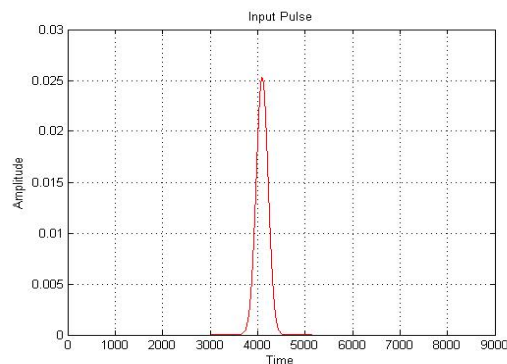


Fig. 2 Graph depicting the optical pulse through the fiber

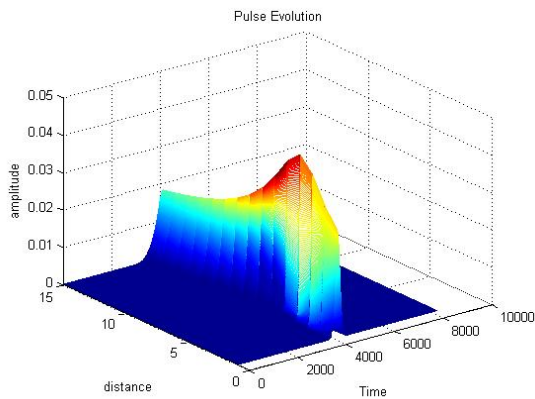


Fig. 3 3D spectrum of the pulse and its variation with time and distance from the optical fiber

Fig. 2 represents a graph depicting the propagation of the optical pulse through the fiber. The standard values of the imaginary value i and π are defined first in the program. Then the attenuation coefficient α is defined and is converted to the linear domain. The standard values for Nonlinearity coefficient (γ), the initial pulse width, the input Chirp parameter, Cubic dispersion coefficient (β_2) and dispersion length are set. The different wavelengths considered range from 700 to 1700 micrometer. The step size is set to 1000 micrometer. Then we initialize a for loop to generate the initial optical field for linearly chirped Gaussian pulses. Subsequently we plot the graph of the input optical pulse with Time (ms) in the X axis and the amplitude (micro meter) in the Y axis.

Fig. 3 depicts the 3D spectrum of the optical pulse and its variation with time and distance from the optical fiber. We use the Fast Fourier Transform and its inverse mostly in the second half of the code. A fast Fourier transform (FFT) is an algorithm which is used for solving the Discrete Fourier transform (DFT) numerically. For vectors, `fftshift(X)` swaps the left and right halves of X. Thus we generate the pulse spectrum using the `fft` and `fftshift` function. Then using the Split Step Fourier Method we calculate the non linear parameter in the middle of the segment rather than at the segment boundary. We also calculate the linear parameter at the beginning and ending of the segment. One more important factor to consider is the Pulse Broadening Ratio (PBR) which is saved at every step size (h) and also the phase of the optical pulse. Thus we can generate the pulse spectrum in 3D and how it varies with Time (ms), Distance travelled (micrometer) and the Amplitude (micrometer).

Using the results of the model proposed we generate two graphs,

1. Loss vs. Wavelength
2. Dispersion vs. Wavelength

B. Simulation of Variation of Loss versus Wavelength

For generating this graph, we define α_0 and λ_0 and then set a range of wavelengths as x. Part of the code proposed

to generate the Loss vs. Wavelength using the results of the model proposed is given.

```
Ralpha=alpha0*((lamda0/0.7)^4);% ghatak and thyagrajan
%page number 41
for i = x(1,2):x(1,1001)
    i = i/1000;
    Ralpha = [Ralpha,alpha0*((lamda0/i)^4)];
    i = i*1000;
end
x = x/1000;
plot(x,Ralpha,'r');
xlabel(' wavelength (micro meter) ----->');
ylabel(' Rayleigh scattering (dB/km) ----->');
grid;
lamda = input('enter the wavelength in micrometer at which
loss is to be calculated = ');
Ralpha = alpha0*((lamda0/lamda)^4);
disp('rayleigh scattering at given wavelength(dB/km)is =');
disp(Ralpha);
```

The variation of Loss vs Wavelength is plotted in Fig. 4.

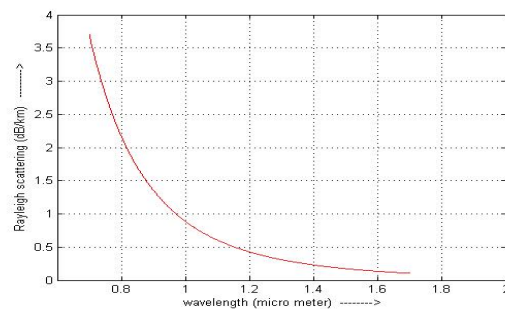


Fig. 4 Graph depicting Loss (Y-Axis) vs. Wavelength (X-Axis)

Taking the same wavelength range from 700 to 1700 micrometers as used in the model proposed, the attenuation coefficient co-efficient due to Rayleigh scattering in fused silica is given by the formula,

$$\alpha(\lambda) = \alpha_0 \left(\frac{\lambda_0}{\lambda} \right)^4$$

where $\alpha_0 = 1.7 \text{ dB/km}$ at $\lambda_0 = 0.85 \mu\text{m}$.

Thus we generate the waveform for the different wavelengths using the results obtained from the first code used for modelling the fibre and plot them in a graph with Wavelength (Micro meter) in the X axis and the loss i.e. Rayleigh scattering (db/km) in the Y axis. The loss at any particular wavelength can also be found by just giving the loss as input after compilation of the program.

The standard Loss vs. Wavelength graph generated for a typical optical fiber by JDS Uniphase Corporation, a company that designs and manufactures products for optical communications is shown.

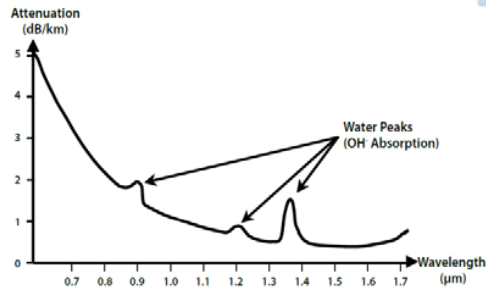


Fig. 5 Fiber attenuation as a function of wavelength for a typical optical fiber [24]

At around the wavelengths of 950, 1244 and 1383nm, the presence of hydrogen and hydroxide ions within the fiber material causes an increase in attenuation. (Water peaks). As we haven't taken this into account, both the graphs are found to be similar without taking the water peaks into consideration. Thus we can state that the model proposed is right.

C. Simulation of Variation of Dispersion with Wavelength

A part of the code proposed to generate the Dispersion vs. Wavelength graph is given.

```
c=3*(10^5); %speed of light in km per sec
n=C0+(C1*(lamda^2))+(C3/((lamda^2)-1))+(C4/(((lamda^2)-1)^2))+(C5/(((lamda^2)-1)^3));
F = diff(n,lamda,2);%differentiation of n wrt lambda, the 3rd
%value that is 2 ,defines the order of differentiation
Lo = 1.1;
int_val = subs(F,lamda,Lo);
Dm = -(1/(Lo*c))*((Lo^2)*int_val)*(10^9);
x=[700:1:1700];
for i = x(1,2):x(1,1001)
    i = i/1000;
    int_val = subs(F,lamda,i);
    Dm=[Dm,-(1/(i*c))*((i^2)*int_val)*(10^9)];%in
%ps/km.nm
    i=i*1000;
end
disp('the zero dispersion wavelength is 1.312 micrometer or
1312 nanometer');
x = x/1000;
Y1=0.0017;
x1=1.31127;
figure(2);
plot(x,Dm,'r');
hold on;
h = stem(x1,Y1,'LineWidth',1);% indicating the cutoff
%wavelength on graph by a stem
set(h,'MarkerFaceColor','red');
hold on;
annotation('textbox', 'Position',[0.5271 0.8976 0.3261 0.0569],
'FitHeightToText','off','BackgroundColor',[1 0.6431 1],
'String',{sprintf('Zero dispersion wavelength is
```

```
1311.27nanometer or 1.31127micrometer')));
hold off;
xlabel('wavelength(micrometer)----->');
ylabel('material dispersion(ps/km.nm)----->');
grid;
Lo=input('enter the operating wavelength in micrometer=');
int_val = subs(F,lamda,Lo);
Dm = -(1/(Lo*c))*((Lo^2)*int_val)*(10^9);
disp('the material dispersion(ps/km.nm)at given wavelength is
=');
```

The variation of Dispersion with Wavelength is plotted in Fig. 6.

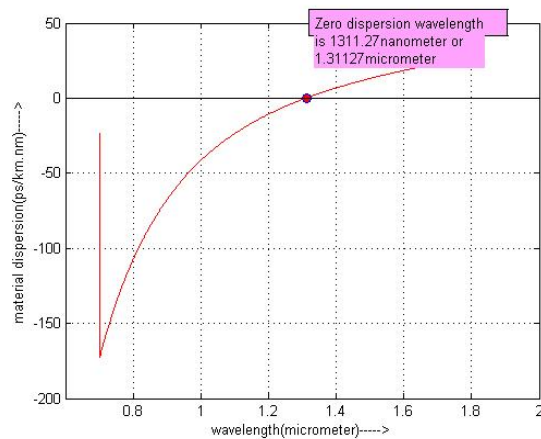


Fig. 6 Graph of Dispersion (Y-Axis) vs. Wavelength (X-Axis)

Fig. 6 shows the variation of dispersion with wavelength of the optical pulses. First we define 5 chromatic dispersion coefficients C_0 , C_1 , C_2 , C_3 , C_4 and C_5 . Then we find the refractive index using the different coefficients. Then we proceed to find the Group velocity dispersion factor F . Then using F and λ we generate a variable called int_val which is used for calculating dispersion for various wavelengths using the formula as given in the code. The zero dispersion wave length is found to be 1.312 micrometer. Thus having found the dispersion for various wavelengths we can plot a graph with Dispersion (ps/km.nm) as the quantity in the X axis and Wavelength (micro meter) as the quantity in the Y axis.

The standard Dispersion vs. Wavelength graph generated for a typical optical fiber by JDS Uniphase Corporation is,

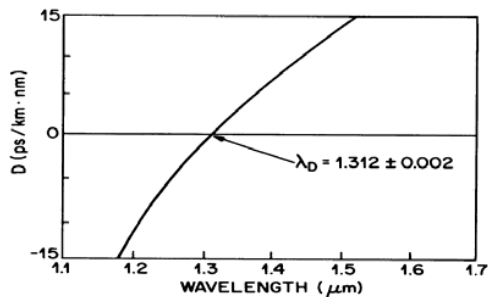


Fig. 7 Measured variation of Dispersion parameter D with Wavelength for a single-mode fiber [24]

On comparing both the graphs, we find both of them to be similar. Thus we can state that the model proposed is right.

VI. CONCLUSION AND FUTURE WORK

Thus an optical fiber was modeled successfully by solving the NLSE using the Split Step Fourier Method. On comparing the graphs generated (Loss vs. Wavelength and Dispersion vs. Wavelength) with the standard graphs obtained by JDS Uniphase Corporation, we find that both are similar thus verifying that the model proposed is right. This is just the beginning in building a Coherent Optical OFDM system. The future scope includes modeling the OFDM transmitter, the RF to Optical up Converter, the Optical to RF down Converter and the OFDM Receiver, which are basically the remaining components of a typical Coherent Optical OFDM System. After modeling all the above mentioned components, an OFDM signal can be transmitted through the optical channel and testing of the transmission speed can be done for bit rates of 100 Giga bits/sec and beyond to test the robustness of the algorithm and the system. Increasing the bit rate decreases Channel Dispersion and other fiber non linearity's thus improving system performance.

Future work involves using an OFDM transceiver with the optical channel to generate an OFDM signal and study its effects for higher bit rates such as 112 Giga bits per second.

REFERENCES

- [1] Shieh, William, Djordjevic and Ivan (2010). OFDM for Optical Communications. USA: Elsevier Academic Press.
- [2] H. Bülow, "Electronic dispersion compensation," presented at the Proc. OFC/NFOEC 2007, Anaheim, CA, Mar. 25–29, 2007, Tutorial, OMG5.
- [3] S. J. Savory, "Digital signal processing options in long haul transmission," presented at the Proc. OFC/NFOEC 2008, San Diego, CA, 2008, Paper, OTuO3.
- [4] B. Spinnler, "Recent advances on polarization multiplexing," presented at the Proc. IEEE Summer Topicals, 2008, TuD2.3
- [5] J. A. C. Bingham, "Multicarrier modulation for data transmission: An idea whose time has come," IEEE Commun. Mag., vol. 28, pp. 5–14, 1990.
- [6] R. van Nee and R. Prasad, OFDM for Wireless Multimedia Communications. Boston: Artech House, 2000.
- [7] W. Y. Zou and Y. Wu, "COFDM: An overview," IEEE Trans. Broadcasting, vol. 41, pp. 1–8, 1995.
- [8] J. M. Kahn and J. R. Barry, "Wireless infrared communications," Proc. IEEE, vol. 85, pp. 265–298, 1997.
- [9] J. B. Carruthers and J. M. Kahn, "Multiple-subcarrier modulation for non directed wireless infrared communication," IEEE J. Sel. Areas Commun., vol. 14, pp. 538–546, 1996.
- [10] O. Gonzalez, R. Perez-Jimenez, S. Rodriguez, J. Rabadan, and A. Ayala, "OFDM over indoor wireless optical channel," IEE Proc.—Optoelectronics, vol. 152, pp. 199–204, 2005.
- [11] J. Armstrong and A. J. Lowery, "Power efficient optical OFDM," Electron. Lett., vol. 42, pp. 370–371, 2006.
- [12] J. Armstrong and B. J. C. Schmidt, "Comparison of asymmetrically clipped optical OFDM and DC-biased optical OFDM in AWGN," IEE Commun. Lett., vol. 12, pp. 343–345, 2008.
- [13] X. Li, R. Mardling, and J. Armstrong, "Channel capacity of IM/DD optical communication systems and of ACO-OFDM," in Proc. ICC '07, 2007, pp. 2128–2133.
- [14] N. Cvijetic, D. Qian, and T. Wang, "10 Giga bits/sec free-space optical transmission using OFDM," presented at the Proc. OFC/NFOEC 2008, San Diego, CA, 2008, Paper, OTHD2.
- [15] S. C. J. Lee, F. Breyer, S. Randel, M. Schuster, J. Zeng, F. Huiskens, H. P. A. van den Boom, A. M. J. Koonen, and N. Hanik, "24-Giga bits/sec transmission over 730 m of multimode fiber by direct modulation of 850-nm VCSEL using discrete multi-tone modulation," presented at the Proc. OFC/NFOEC 2007, Anaheim, CA, Mar. 25–29, 2007, Paper PDP6.
- [16] S. C. J. Lee, F. Breyer, S. Randel, O. Ziemann, H. P. A. van den Boom, and A. M. J. Koonen, "Low-cost and robust 1-Gbit/s plastic optical fiber link based on light-emitting diode technology," presented at the Proc. OFC/NFOEC 2008, San Diego, CA, 2008, Paper, OWB3
- [17] N. Cvijetic and W. Ting, "WiMAX over free-space optics—Evaluating OFDM multi-subcarrier modulation in optical wireless channels," in Proc. IEEE Sarnoff Symp., Princeton, NJ, USA, 2006.
- [18] J. M. Tang, P. M. Lane, and K. A. Shore, "Transmission performance of adaptively modulated optical OFDM signals in multimode fiber links," IEEE Photon. Technol. Lett., vol. 18, pp. 205–207, 2006.
- [19] B. J. C. Schmidt, A. J. Lowery, and J. Armstrong, "Experimental demonstrations of electronic dispersion compensation for long haul transmission using direct-detection optical OFDM," J. Lightw. Technol., pp. 196–203, 2008.
- [20] A. J. Lowery and J. Armstrong, "Orthogonal-frequency-division multiplexing for dispersion compensation of long-haul optical systems," Opt. Expr., vol. 14, pp. 2079–2084, 2006.
- [21] W. Shieh and C. Athaudage, "Coherent optical orthogonal frequency division multiplexing," Electron. Lett., vol. 42, pp. 587–588, 2006.
- [22] S. L. Jansen, I. Morita, N. Takeda, and H. Tanaka, "20-Giga bits/sec OFDM transmission over 4,160-km SSMF enabled by RF-pilot tone phase noise compensation," presented at the Proc. OFC/NFOEC 2007, Anaheim, CA, Mar. 25–29, 2007, Paper PDP15.
- [23] Le Nguyen Binh, 'MATLAB Simulink Simulation Platform for Photonic Transmission Systems'. I. J. Communications, Network and System Sciences., pp 91-168, May.2009
- [24] Brandon Collings, Fred Heismann, Gregory Lietaert, Reference Guide to Fiber Optic Testing, California, USA; JDS Uniphase Corporation 2010.